

# Domain wall traps for low-field switching of sub-micron elements

R. D. McMichael\*, J. Eicke†, M. J. Donahue\* and D. G. Porter\*

\*National Institute of Standards and Technology, Gaithersburg, MD 20899

† Institute for Magnetism Research, The George Washington University, Washington, DC 20052

In magnetic random access memory (MRAM), power consumption depends on the coercivity of the magnetic elements in the memory cells. In this paper a new method is described that uses a “domain wall trap” element shape to reduce both the coercivity and the dependence of coercivity on element size in submicron magnetic elements. Micromagnetic simulations of a shaped Permalloy element show coercivity less than one tenth the coercivity calculated for a rectangular Permalloy element of the same size. The switching times for the domain wall traps are shown to be comparable to those of rectangular elements.

## I. INTRODUCTION

A low switching field and reproducible switching behavior are desirable properties of MRAM cells. The low switching field reduces the power consumed and dissipated by the cell, and the reproducible switching behavior simplifies writing and read back of information stored in the cell.

In rectangular cells it has been found that magnetization reversal occurs by expansion of domains that form at the ends of the cell. Because of the symmetry of the rectangle, the end domains can be in a number of different magnetization states in zero field. Therefore, the switching field may be history-dependent<sup>1</sup>. The miniaturization of rectangular cells also faces the problem that the coercivity of rectangular cells is inversely proportional to width<sup>2,3</sup>.

To overcome the problem of irreproducible switching in rectangular cells, cells with tapered ends have been proposed that nucleate reversals in the middle rather than at the ends of the cells. Although the tapered-cells are found to allow more reliable switching than the rectangular cells, it is found that the tapered-cells have a higher coercivity than the rectangular cells<sup>4</sup>.

Because reversal in both rectangular and tapered-end strips often involves propagation of domain walls, the equilibrium properties of head-to-head walls in thin magnetic strips may provide insight into the switching behavior of rectangles and other shapes. Micromagnetic calculations of head-to-head walls show that the energy of transverse and vortex head-to-head domain walls both increase with with increasing strip width<sup>5</sup>.

In this paper, the width-dependence of the energy of transverse head-to-head domain walls is used to construct a domain wall trap. The following describes the important design features and computed switching fields and

switching times for domain wall traps, including computational demonstrations of the dramatically reduced switching field and comparable switching times of domain wall traps when compared to rectangular elements.

## II. THE DOMAIN WALL TRAP

The domain wall trap geometry, illustrated in Fig. 1, consists of a narrow central section connected to wider end sections by sections tapered asymmetrically about the  $x$ -axis. The outer ends of the end sections may be similarly asymmetrically tapered, or a series of domain wall traps may be attached end-to-end. The asymmetry of the tapered sections enables initialization of a single head-to-head wall in the center section of the trap when a large initialization field is applied in the plane of the film perpendicular to the long axis of the element. Because the magnetostatic energy is locally minimized when the magnetization lies parallel to edges, the magnetization will be directed inward (outward) as the initialization field is reduced from large values in the  $+y$  ( $-y$ ) direction, leaving a domain wall in the center section. The case of outward directed magnetization is shown in Fig. 2a.

For the calculations described below, we have masked the effects of the element ends by embedding the domain wall trap in an infinitely long strip. See Fig. 1c. We anticipate that the effects of finite ends can be accounted for by superposing the magnetostatic fields due to the end structures. Furthermore, we have found that isolated domain wall traps having tapered ends have behavior that is qualitatively similar to the embedded domain wall trap behavior.

Under the influence of a relatively small applied field, the initialized domain wall can be made to move through the center section of the trap. Because the domain wall energy increases with strip width, the tapered sections provide a force that can prevent the domain wall from propagating off the end of the element. If this force is not exceeded by the force due to the applied field, the domain wall will be preserved for switching to the opposite end of the element.

As will be described below, the minimum energy positions of the domain wall in the trap are at the ends of the center region, so that a finite field is required to switch the magnetization.

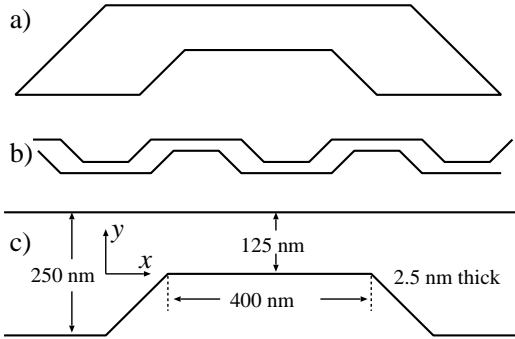


FIG. 1. a) The shape of a stand alone domain wall trap. b) A series of domain wall traps connected as a long magnetic strip. c) The dimensions of the domain wall trap used in much of the paper.

### III. CALCULATION TECHNIQUE

Calculations were done using a micromagnetic model, OOMMF, developed at NIST<sup>6</sup>. The model includes the effects of the exchange energy, characterized by the exchange stiffness constant,  $A$ , the magnetostatic energy, characterized by the spontaneous magnetization,  $M_s$ , and an applied field energy. For most calculations in this paper,  $A$  and  $M_s$  were taken to mimic  $\text{Ni}_{80}\text{Fe}_{20}$  with  $A = 1.3 \times 10^{-11}$  J/m and  $M_s = 8.0 \times 10^5$  A/m. Magnetocrystalline anisotropy is neglected. The in-plane cell size was  $5 \text{ nm} \times 5 \text{ nm}$  for all calculations and out-of-plane thicknesses of 5 nm and 2.5 nm were used.

We have assumed that the magnetization is uniform across the thickness of the film to allow the use of a two-dimensional grid. The spins are free to rotate in three dimensions, but the large magnetostatic energy required to tilt the spins out of the plane results in predominantly in-plane spin configurations. Coupled with a domain wall width that is much greater than the thickness of the sample, the result is good conformity with the assumption of a uniform magnetization across the thickness of the film.

The exchange field was calculated using an eight-neighbor cosine scheme<sup>7</sup> and the magnetostatic field was calculated using a technique that assumes a constant magnetization within grid cells and calculates the magnetostatic field at the center of each cell due to surface charges at the cell boundaries<sup>8</sup>. The semi-infinite ends of the strip are simulated by adding magnetostatic charge at the ends of the calculation region to represent the charge at the ends of the uniformly magnetized semi-infinite regions, effectively canceling the magnetostatic charge on the ends of the calculated region. The geometry of the embedded domain wall trap is shown in Fig. 1c.

The magnetization was relaxed according to Landau-Lifshitz damping,  $d\mathbf{M}/dt = -|\gamma|(\mathbf{M} \times \mathbf{H}_{\text{eff}}) - \frac{\lambda}{M_s} \mathbf{M} \times (\mathbf{M} \times \mathbf{H}_{\text{eff}})$ , where  $\mathbf{H}_{\text{eff}}$  includes the demagnetizing field, the applied field and the exchange field. The damping parameter,  $\lambda/\gamma = 0.02$ . The magnetization was allowed to precess until the maximum value of  $(\mathbf{M} \times \mathbf{H}_{\text{eff}})/M_s^2$  for all cells was less than  $1.0 \times 10^{-5}$ .

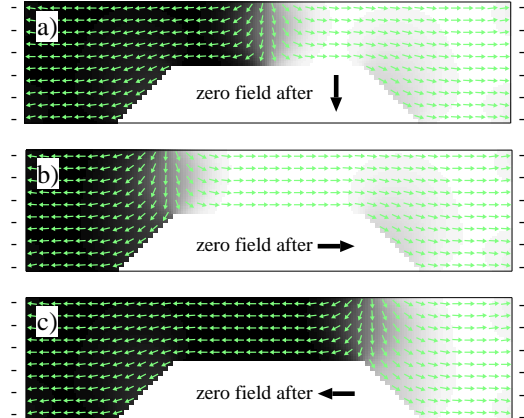


FIG. 2. Spin configurations at zero applied field. a) Unstable state after initialization in the  $-y$  direction. b) and c) show stable configurations after application of a field in the  $+x$  and  $-x$  directions, respectively.

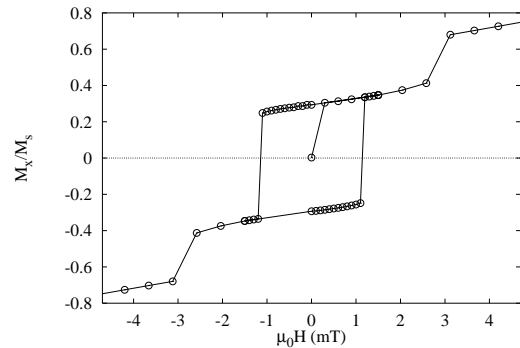


FIG. 3. A hysteresis loop for an embedded domain wall trap. The central region of the trap is  $125 \text{ nm} \times 400 \text{ nm} \times 2.5 \text{ nm}$  thick. The switching field for the domain wall in the trap is 1.1 mT and the domain wall is pushed out of the trap with a field of 3.2 mT.

### IV. RESULTS

Zero-field spin configurations for the embedded domain wall trap are shown in Fig. 2, which shows an unstable configuration following initialization, and two stable configurations with the domain wall at either end of the trap.

Reduction of exchange energy of the domain wall when it is at either end of the trap plays a large role in stabilizing the wall at the trap ends. In the unstable configuration in Fig. 2a, the spins along the lower edge of the center region form a  $180^\circ$  domain wall. In contrast, the spins along the lower edge in Figs. 2b) and c) turn through only  $135^\circ$  when the domain wall rests at the interior corner of the trap.

The hysteresis loop for the shaped element is shown in Fig. 3. After initialization, the element has  $\langle M_x \rangle = 0$  with the wall unstably located in the center of the sample (Fig. 2a). When a small field is applied in the  $+x$  direction, the domain wall propagates to the left end of the trap, increasing the size of the domain oriented in the  $+x$

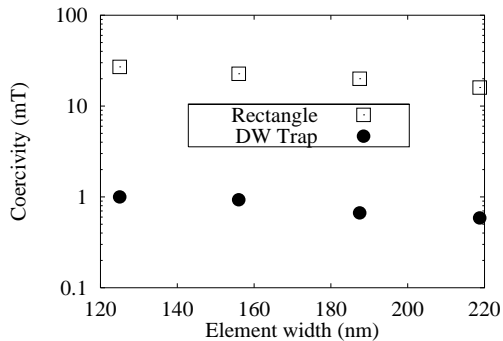


FIG. 4. The effect of size on coercivity for a domain wall trap and for a rectangular element sized to fit in the center region of the domain wall trap. In the case of the domain wall trap, the element width refers to the width of the center region. The coercive field for the rectangular element is an order of magnitude higher.

direction. Once the domain wall has arrived at its energy minimum location at the end of the trap, a field of -1.1 mT is required to move the domain wall to the other end of the trap. The field required to move the domain wall out of the trap is 3.2 mT. The susceptibility indicated by the nonzero slope of the hysteresis loop is due to motion of the domain wall in the local energy minima at the trap ends.

For comparison with the domain wall trap, a rectangular element was chosen with the same size as the central region of the domain wall trap, referred to below as a “central rectangle.” The central rectangle is chosen because it defines the region that is reversed in the domain wall trap and is the active region of the cell. The coercive fields of domain wall traps and the central rectangles are shown in Fig. 4. The switching fields of the domain wall traps are much smaller than the coercivities of the central rectangles. Even comparing the largest rectangle with the smallest domain wall trap, which have about the same overall size, the rectangle has a coercivity about sixteen times the coercivity of the domain wall trap.

The large reduction in switching field achieved by the domain wall trap is very significant for applications that would benefit from low power consumption. For example, assuming that the applied fields are generated by current flowing in a nearby wire with constant resistance, a tenfold reduction in switching field requires 10% of the current, and only 1% of the power to switch.

The switching speed may also be important for a number of applications. Switching times for a shaped element and a central rectangle are compared in Fig. 6. The field is applied instantaneously; the switching time,  $t_0$ , is defined as the time required for  $\langle M_x \rangle$  to pass through zero. There is an additional ‘ring-down’ time for both the domain wall trap and rectangular element that is on the order of 1 ns. The switching times are the same order of magnitude, but the domain wall trap switches with much less applied field. Both the rectangle and the do-

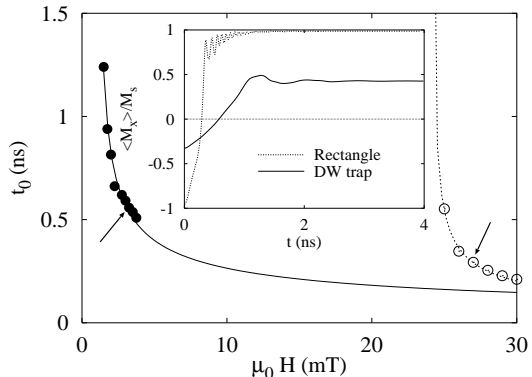


FIG. 5. Switching times for the domain wall trap (filled circles) and the central rectangle (open circles) versus applied field. The switching time,  $t_0$ , is the time required for the average magnetization to pass through zero. The solid lines are fits to  $t_0 = a/[\mu_0(H - H_0)]^{1/2}$ . The arrows indicate the applied fields used for the plots of  $\langle M_x(t) \rangle$  shown in the inset.

main wall trap switch faster with increased applied field, but the domain wall trap switching speed is limited by the fact that with too much field, the domain wall can be ejected from the trap. Such a limitation may be avoidable with pulsed applied fields, timed to turn off before the wall reaches the end of the trap.

The switching times fit curves of the form  $t_0 = a/[\mu_0(H - H_0)]^{1/2}$ , with  $a = 0.79 \text{ ns}/(\text{mT})^{1/2}$ ,  $\mu_0 H_0 = 1.1 \text{ mT}$  for the domain wall trap and  $a = 0.49 \text{ ns}/(\text{mT})^{1/2}$ ,  $\mu_0 H_0 = 24.2 \text{ mT}$  for the rectangle. For a given amount of field in excess of the critical field, the rectangle switched almost twice as fast as the domain wall trap. It is interesting to note that the dynamic reversal patterns of the rectangle involve motion of two domain walls compared to the motion of only one domain wall in the reversal of a domain wall trap.

- 
- <sup>1</sup> B.A. Everitt, A.V. Pohm, R.S. Beech, A. Fink, J.M. Daughton, *IEEE Trans. Magn.*, **34**, 1060, (1995).
  - <sup>2</sup> J. Gadbois and J.-G. Zhu, *IEEE Trans. Magn.*, **31**, 3802, (1995).
  - <sup>3</sup> Jing Shi, S. Tehrani, T. Zhu, Y.F. Zheng and J.-G. Zhu, *Appl. Phys. Lett.* **74**, 2525, 1999.
  - <sup>4</sup> J. Gadbois, J.-G. Zhu, W. Vavra, A. Hurst *IEEE Trans. Magn.* **34**, 1066, 1998.
  - <sup>5</sup> R. D. McMichael and M. J. Donahue, *IEEE Trans. Magn.* **33**, 4167, 1997.
  - <sup>6</sup> <http://math.nist.gov/oommf>
  - <sup>7</sup> M.J. Donahue and R.D. McMichael, *Physica B* **233**, 272, 1997.
  - <sup>8</sup> R.D. McMichael, M.J. Donahue, D.G. Porter, and J. Eicke *J. Appl. Phys.* **85**, 5816, 1999.